Progress In Electromagnetics Research, PIER 45, 243–262, 2004

MODAL METHOD ANALYSIS OF MULTILAYERED COATED CIRCULAR WAVEGUIDE USING A MODIFIED CHARACTERISTIC EQUATION

F.-G. Hu, C.-F. Wang, Y. Xu, and Y.-B. Gan

Temasek Laboratories
National University of Singapore
10 Kent Ridge Crescent, Singapore 119260

Abstract—In this paper, the modal method is applied to analyze coated circular waveguide terminated by a perfect electric conductor (PEC) plate. The key to this method is the accurate calculation of the propagation constants of modes in coated circular waveguide. To overcome numerical difficulties, such as overflow, encountered in solving characteristic equation, the characteristic equation is modified using Hankel function of the second kind instead of Bessel function of the first kind in the coated layers. The modified characteristic equation can be accurately solved to obtain the propagation constants even for very large circular waveguide with highly lossy coatings. To verify the modified characteristic equation, the attenuation and scattering property of circular waveguide structure have been simulated. Simulation results agree well with the reference results.

1 Introduction

2 Characteristic Equation and its Modification

3 Scattering Analysis of Circular Coated Waveguide

4 Numerical Results

5 Conclusions

References

1. INTRODUCTION

Coated circular waveguide structure has been studied over the years due to its good electromagnetic property and wide applications to scattering problems and circuits design. As mentioned in [1], the air intake can be modeled as an open-ended circular waveguide terminated at one end with a perfect electric conductor (PEC), which simulates the engine blades. This model is a simple-minded approximation of the practical model. Rigorous modal analysis of the coated circular waveguide can help us figure out the field inside the cavity and pinpoint the type of material that is most effective in the reduction of scattering. The accurate and fast solution of circular waveguide structure can also be used to verify newly developed numerical methods and characterize the electromagnetic property of newly developed materials, such as nano-materials.

Through the extensive investigation of many researchers, various methods have been developed to simulate the circular waveguide structure, including the modal method [1–4], the shooting and bouncing ray (SBR) method [5, 6], the Generalized Ray Expansion (GRE) method [7], iterative physical optics (IPO) method, progressive physical optics (PPO) method [8], method of moment (MoM) [9, 10], and fast finite element method (FEM) [11]. The SBR method lacks accuracy at lower frequency and fails at caustics, but it can be used for general-purpose calculations. The GRE method overcomes the disadvantage of the SBR by subdividing the aperture into smaller subapertures. The IPO method provides accurate results, even for deep cavities, with moderate computational complexity. The numerical techniques (MoM, FEM, and their combination) can treat arbitrarily shaped three-dimensional cavities when the cavities are small. The fast FEM can be used for the analysis of large cavities.

In this paper, the modal method is applied to analyze coated circular waveguide terminated by a perfect electric conductor (PEC) plate. The reason for choosing the modal method is its accuracy and efficiency in analyzing circular waveguide structures. The key to this method is the accurate calculation of the propagation constants of modes in coated circular waveguide. To overcome numerical difficulties, such as overflow, encountered in solving characteristic equation [12, 13], the characteristic equation is modified using the Hankel function of the second kind, instead of Bessel function of the first kind in the coated layers. The modified characteristic equation can be accurately solved to obtain the propagation constants even for very large circular waveguide with highly lossy coatings. To verify the modified characteristic equation, the attenuation and scattering property of the circular waveguide structure have been simulated. Simulation results agreed well with the reference results.

2. CHARACTERISTIC EQUATION AND ITS MODIFICATION

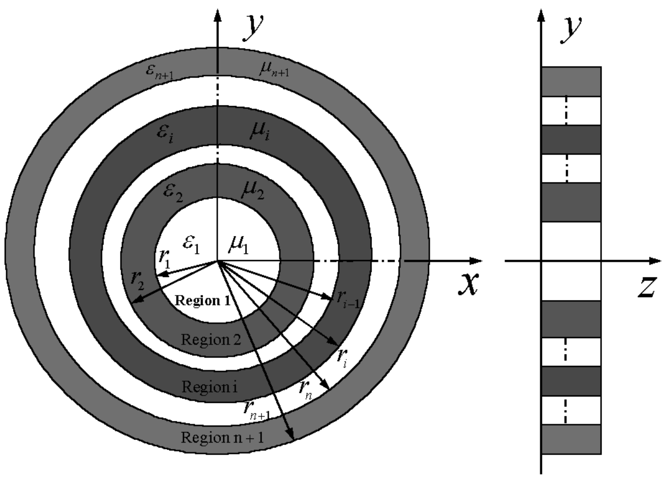

Figure 1. Exaggerated cross-sectional view of multilayered coated waveguide.

Figure 1 shows an exaggerated view of the coating layers to illustrate the geometrical features of the circular waveguide as in [12]. In real applications, the coating layers will be very thin relative to the diameter of the guide. The waveguide walls are assumed to be perfectly conducting. The characteristic equation for modes' propagation constants is derived from the well-known method of seeking nontrivial solution of the coefficients in the field expressions of the equations obtained by enforcing the continuity of the four tangential fields at each interface between two layers. The z-components of the electric and magnetic vector potential (ψ_j^e and ψ_j^m, $j = 1, 2, \ldots, n+1$ denotes the index of the region) in each layer must satisfy the Helmholz equation and the tangent components of electric fields, derived from ψ_j^e and ψ_j^m, must vanish on the waveguide wall. The characteristic equation for the coated circular waveguide shown in Fig. 1 can be expressed as follows

[12],

$$\det\begin{bmatrix} \frac{k_{\rho 1}^2}{\varepsilon_1}F_1(r_1) & 0 & -m_{11} & -m_{12} \\ 0 & \frac{k_{\rho 1}^2}{\mu_1}F_1(r_1) & -m_{21} & -m_{22} \\ k_{\rho 1}F_1'(r_1) & \frac{mk_z}{\omega\mu_1 r_1}F_1(r_1) & -m_{31} & -m_{32} \\ \frac{mk_z}{\omega\varepsilon_1 r_1}F_1(r_1) & k_{\rho 1}F_1'(r_1) & -m_{41} & -m_{42} \end{bmatrix} = 0 \qquad (1)$$

The detailed derivation of the characteristic equation (1) can be found in [12]. As mentioned in [12] and [14], m_{ij} refers to the element in row i and column j of a 4×4 matrix $M = M_{2,1}M_{2,2}^{-1}M_{3,2}\cdots M_{n,n}^{-1}M_{n+1,n}$, in which $M_{a,b}$ indicates the matrix resulted from the tangential fields in region a matched at boundary r_b. The m_{ij} is a function of $F_i(\rho)$, $G_i(\rho)$, $K_1(\rho)$, $K_2(\rho)$, and their derivatives. These components can be expressed as follows:

$$\begin{aligned}
F_i(\rho) &= J_m(k_{\rho i}\rho), \quad F_i'(\rho) = J_m'(k_{\rho i}\rho), \ 1 \le i \le n \\
G_i(\rho) &= N_m(k_{\rho i}\rho), \quad G_i'(\rho) = N_m'(k_{\rho i}\rho), \ 2 \le i \le n \\
K_1(\rho) &= J_m(k_{\rho\,\mathrm{n}+1}\rho)N_m(k_{\rho\,\mathrm{n}+1}r_{n+1}) - N_m(k_{\rho\,\mathrm{n}+1}\rho)J_m(k_{\rho\,\mathrm{n}+1}r_{n+1}) \\
K_1'(\rho) &= J_m'(k_{\rho\,\mathrm{n}+1}\rho)N_m'(k_{\rho\,\mathrm{n}+1}r_{n+1}) - N_m'(k_{\rho\,\mathrm{n}+1}\rho)J_m(k_{\rho\,\mathrm{n}+1}r_{n+1}) \\
K_2(\rho) &= J_m(k_{\rho\,\mathrm{n}+1}\rho)N_m'(k_{\rho\,\mathrm{n}+1}r_{n+1}) - N_m(k_{\rho\,\mathrm{n}+1}\rho)J_m'(k_{\rho\,\mathrm{n}+1}r_{n+1}) \\
K_2'(\rho) &= J_m'(k_{\rho\,\mathrm{n}+1}\rho)N_m'(k_{\rho\,\mathrm{n}+1}r_{n+1}) - N_m'(k_{\rho\,\mathrm{n}+1}\rho)J_m'(k_{\rho\,\mathrm{n}+1}r_{n+1})
\end{aligned}$$

$$k_{\rho i}^2 + k_z^2 = k_i^2, \quad k_i^2 = \omega^2\mu_i\varepsilon_i, \quad 1 \le i \le n+1$$

J_m is the Bessel function of the first kind of order m, N_m is the Bessel function of the second kind of order m.

It is noted that the characteristic equation (1) in [12] cannot be directly used to determine the k_z for large circular waveguide with highly lossy coatings numerically, due to the limitation of computer precision. We will consider the characteristic equation in detail by a special case. As mentioned in [12], in region $n+1$, the characteristic equation involves one term $K_1(r_n) = J_m(\chi_1)N_m(\chi_2) - N_m(\chi_1)J_m(\chi_2)$, in which $\chi_1 = k_{\rho\,\mathrm{n}+1}r_n$, $\chi_2 = k_{\rho\,\mathrm{n}+1}r_{n+1}$. Let $P_1 = J_m(\chi_1)N_m(\chi_2)$ and $P_2 = N_m(\chi_1)J_m(\chi_2)$. In the case of $\mathrm{Im}(k_{\rho\,\mathrm{n}+1}) < 0$, both P_1 and P_2 will be very large, as $|\mathrm{Im}(\chi_1)|$ and $|\mathrm{Im}(\chi_2)|$ increases (for example, more than 20). Figure 2 shows the real and imaginary parts of P_1 and P_2 as a function of the imaginary part of χ_2. From Fig. 2, it is obvious that these two large numbers P_1 and P_2 are deemed to be equal within the

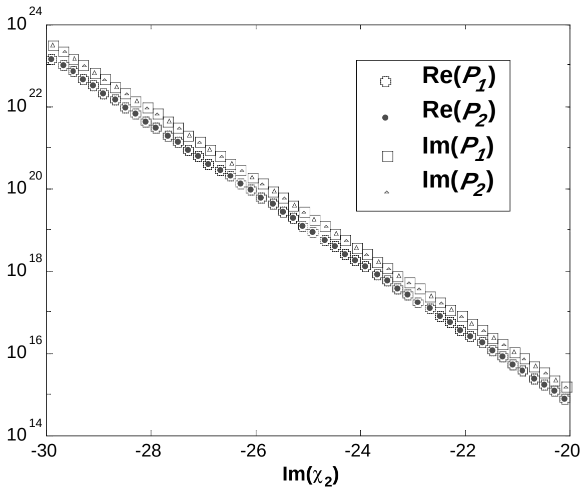

Figure 2. The real and imaginary parts of P_1 and P_2 as a function of the imaginary part of $\chi_2 : \mathrm{Re}(\chi_2) = 3.0,\ r_1/r_2 = 99\%$, and $m = 1$.

range of computer precision. As a result, P_1 minus P_2 calculated using computer will leave a random value that will numerically distort the characteristic equation. In order to accurately solve the characteristic equation numerically using computer, the large parts contained in the characteristic equation must be offset before programming. In fact, one can obtain a numerically stable formula using expression of Bessel function, given as follows,

$$\begin{aligned} K_1(r_n) &= J_m(\chi_1)N_m(\chi_2) - N_m(\chi_1)J_m(\chi_2) \\ &= [iN_m(\chi_1) + H_m(\chi_1)]N_m(\chi_2) - N_m(\chi_1)[iN_m(\chi_2) + H_m(\chi_2)] \\ &= H_m(\chi_1)N_m(\chi_2) - N_m(\chi_1)H_m(\chi_2) \end{aligned} \tag{2}$$

in which H_m is the Hankel function of the second kind of order m. Let $MP_1 = H_m(\chi_1)N_m(\chi_2)$ and $MP_2 = N_m(\chi_1)H_m(\chi_2)$. Figure 3 shows the real and imaginary parts of MP_1 and MP_2 as a function of the imaginary part of χ_2. From the Fig. 3, it is observed that $K_1(r_n)$ can be more accurately calculated using the modified formula $K_1(r_n) = MP_1 - MP_2$, as MP_1 and MP_2 are of the same order of magnitude. The formula (2) shows that the numerically calculable expression using computer can be obtained by substituting the Bessel function of the first kind, J_m, with the Hankel function of the second kind, H_m. In addition, the derivative of J_m should be changed correspondingly into that of H_m. Figure 4 shows propagation constants $k_z r_2$ in a circular waveguide coated with one-layer material ($\varepsilon_{r2} =$

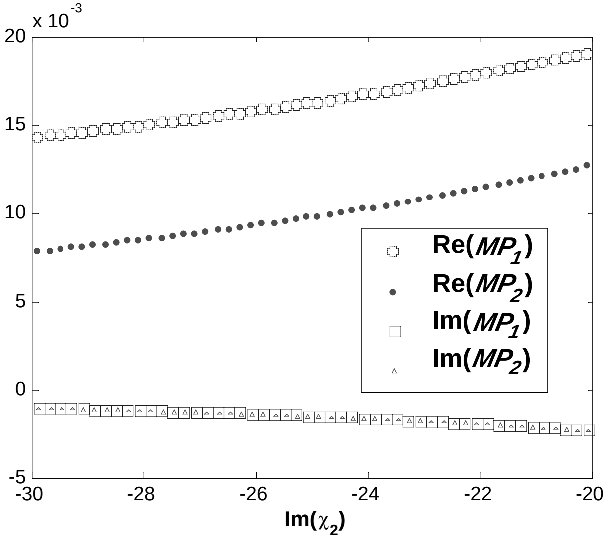

Figure 3. The real and imaginary parts of MP_1 and MP_2 as a function of the imaginary part of χ_2 : $\mathrm{Re}(\chi_2) = 3.0$, $r_1/r_2 = 99\%$, and $m = 1$.

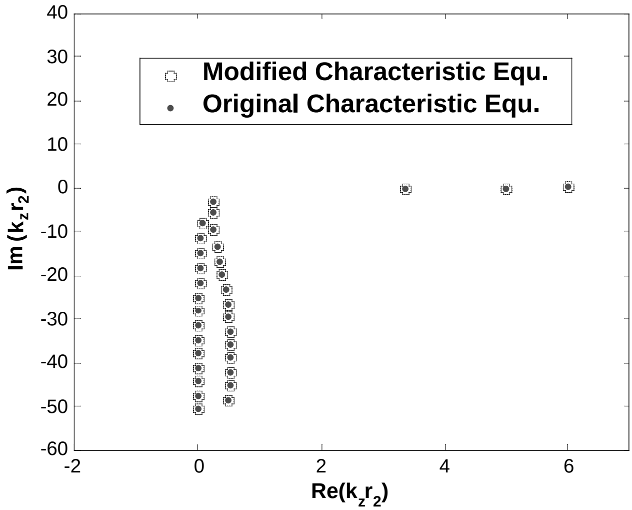

Figure 4. The propagation constants $k_z r_2$ in a circular waveguide coated with one-layer material: $\varepsilon_{r2} = 1.0$, $\mu_{r2} = 1.5 - j2.0$, $r_2/\lambda = 1.0$, and $r_1 = 0.99 r_2$.

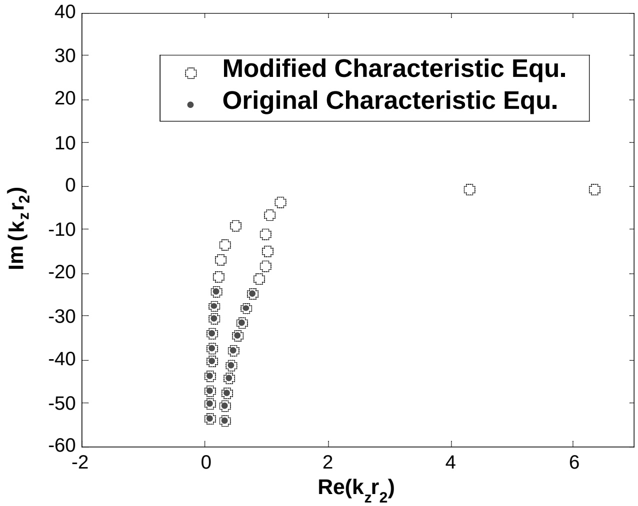

Figure 5. The propagation constants $k_z r_2$ in a circular waveguide coated with one-layer material: $\varepsilon_{r2} = 1.0$, $\mu_{r2} = 1.5 - j5.0$, $r_2/\lambda = 1.5$, and $r_1 = 0.99r_2$.

1.0, $\mu_{r2} = 1.5 - j2.0, r_2/\lambda = 1.0$, and $r_1 = 0.99r_2$) obtained using the original and modified characteristic equations. The two characteristic equations can produce all the propagation constants in almost the same accuracy. When the cross-section of the circular waveguide becomes larger (in wavelength) and the coating materials are more lossy, some roots of the characteristic equation will be lost using the original characteristic equation. The entire set of roots can be found using the modified characteristic equation. This can be clearly observed in Fig. 5. The characteristic equation for the multi-layer coated waveguide ($n+1 > 2$) can be easily modified by using H_m and its derivative instead of J_m and its derivative in region i ($1 < i < n+1$), respectively. The modified characteristic equation will enable us to accurately find all propagation constants in the multi-layer ($n+1 > 2$) coated waveguide.

In the coated circular waveguide, there are no longer pure TM and TE modes, with exception of the case with $m = 0$. The normal modes in the waveguide are commonly classified into EH_{mn} and HE_{mn} in such way that in the limiting case of a vanishing thin coating [12],

$$HE_{mn} \to TE_{mn} \quad \text{and} \quad EH_{mn} \to TM_{mn}. \tag{3}$$

After determination of the propagation constants, the modal field can be calculated using the procedure described in [12].

3. SCATTERING ANALYSIS OF CIRCULAR COATED WAVEGUIDE

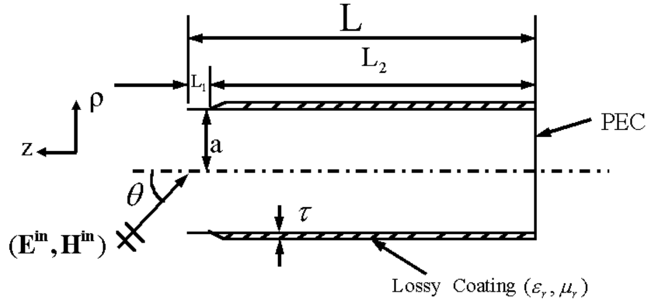

Figure 6. Coated waveguide illuminated by a plane wave.

Figure 6 shows a circular coated waveguide terminated by a PEC plate. The coating material is lossy. The basic steps for the evaluation of the scattering cross section from a coated waveguide are similar to those of the uncoated waveguide. The difference between them is that the normal modes in the coated waveguide attenuate as they propagate. As mentioned in [1], in the following calculations, we make two approximations: (i) the normal modes excited in the short uncoated portion of the waveguide are the same as those encountered in the previous uncoated guide, and (ii) the normal modes propagate from the waveguide without any reflection or mode conversion. When the length of the uncoated region near the waveguide opening is sufficiently long ($> \lambda/2$), the transmission of the incoming wave into the waveguide is not affected by the presence of the coating and the assumption (i) above will be satisfied. If the frequency is not too high and the thickness of coating is gradually increased, the reflection of the transmitted normal mode is not significant [15] and the mode conversion is not critical, which is the requirement of the assumption (ii) mentioned above. Note the mode conversion is more significant at a higher frequency [16]. For the interior irradiation, the propagation factors should be modified, namely [1]

$$e^{-j\gamma 2L} \Rightarrow e^{-j2(\gamma L_1+\overline{\gamma} L_2)} \tag{4}$$

where L_1, and L_2 are the lengths of the uncoated and coated regions of the waveguide, respectively. The bar over the propagation constant indicates that of the coated waveguide.

4. NUMERICAL RESULTS

An in-house code using the modified characteristic equation has been implemented for calculating the propagation constants in the multilayered coated circular waveguide. The in-house code can also be used to simulate the scattering from coated circular waveguide structure shown in Fig. 6. The Muller's method is applied to find the roots of the characteristic equation. In order to avoid the loss of the roots that correspond to the important modes, the initial values of the roots scan the interesting region in the complex plane.

The propagation constants of the HE_{11}, HE_{12}, and EH_{11} modes in the circular coated waveguide shown in Fig. 7 are given in Figs. 8–10. The results from our code are compared to the results available in [12].

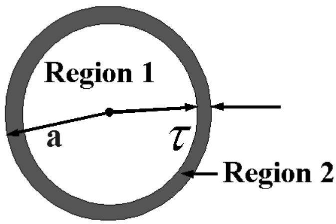

Figure 7. A lossy magnetic coated waveguide with $\varepsilon_r = 1.0$, $\mu_r = 1.5 - j2.0$.

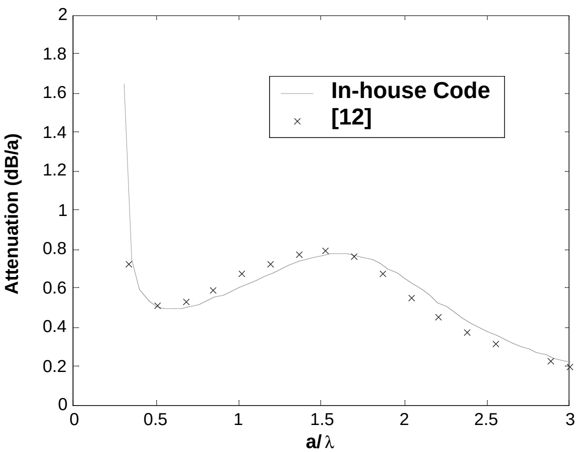

(a) $\tau/a = 1\%$

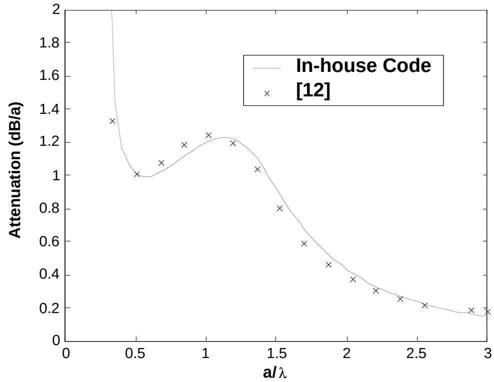

(b) $\tau/a = 2\%$

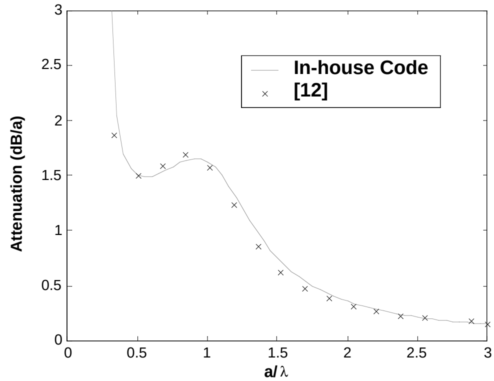

(c) $\tau/a = 3\%$

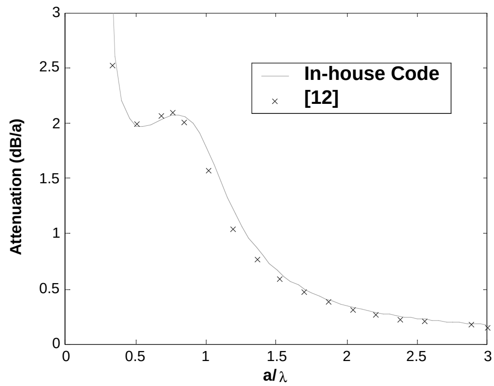

(d) $\tau/a = 4\%$

Figure 8. Attenuation constants of HE_{11} mode.

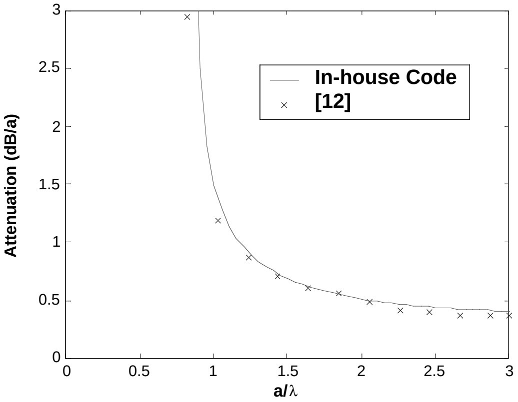

(a) $\tau/a = 1\%$

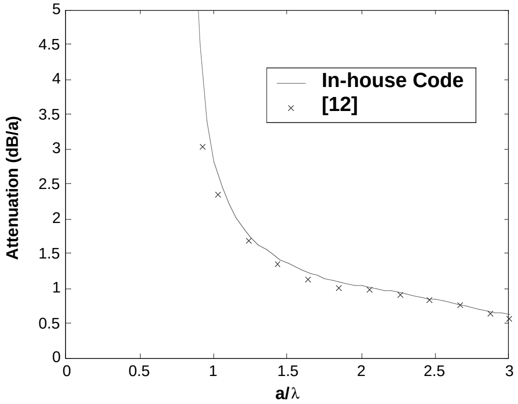

(b) $\tau/a = 2\%$

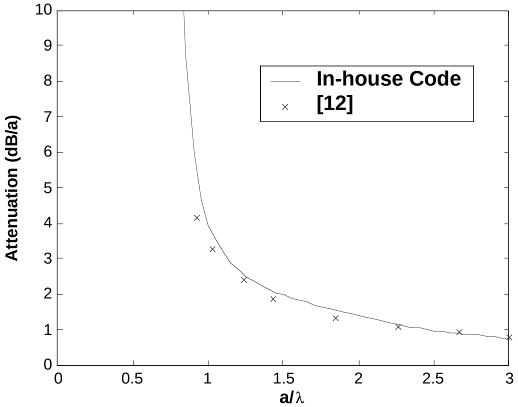

(c) $\tau/a = 3\%$

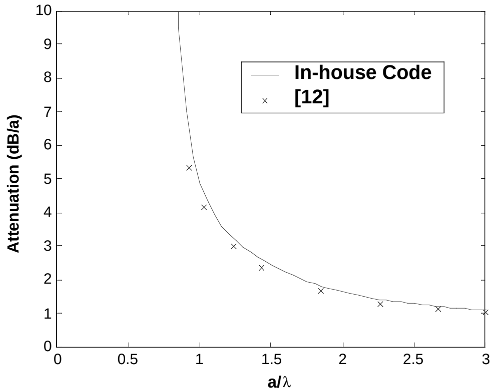

(d) $\tau/a = 4\%$

Figure 9. Attenuation constants of HE_{12} mode.

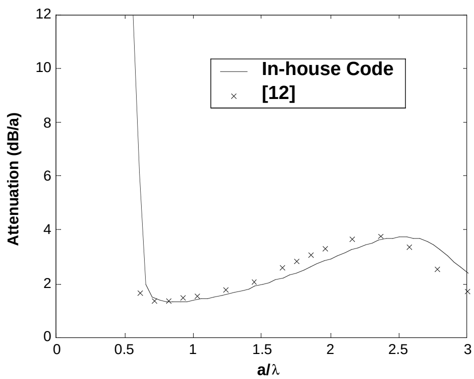

(a) $\tau/a = 1\%$

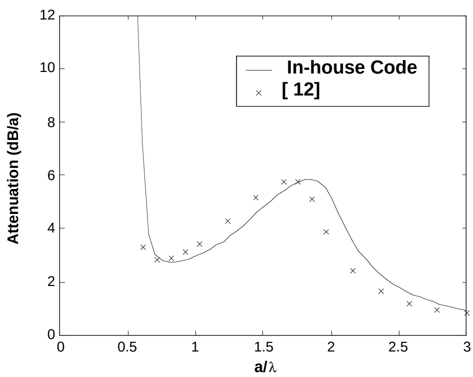

(b) $\tau/a = 2\%$

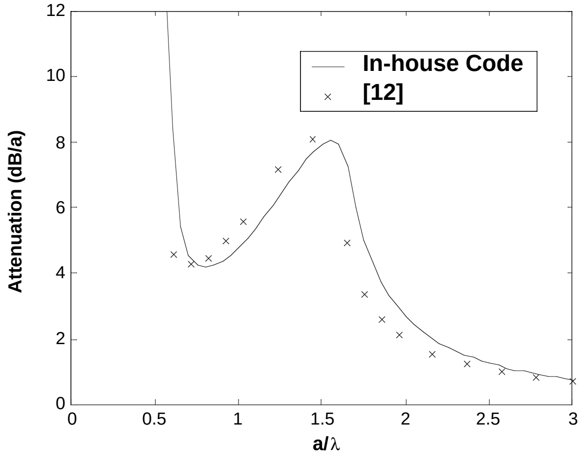

(c) $\tau/a = 3\%$

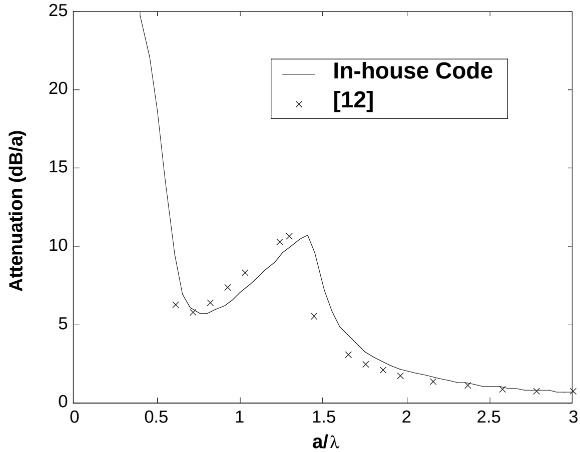

(d) $\tau/a = 4\%$

Figure 10. Attenuation constants of EH_{11} mode.

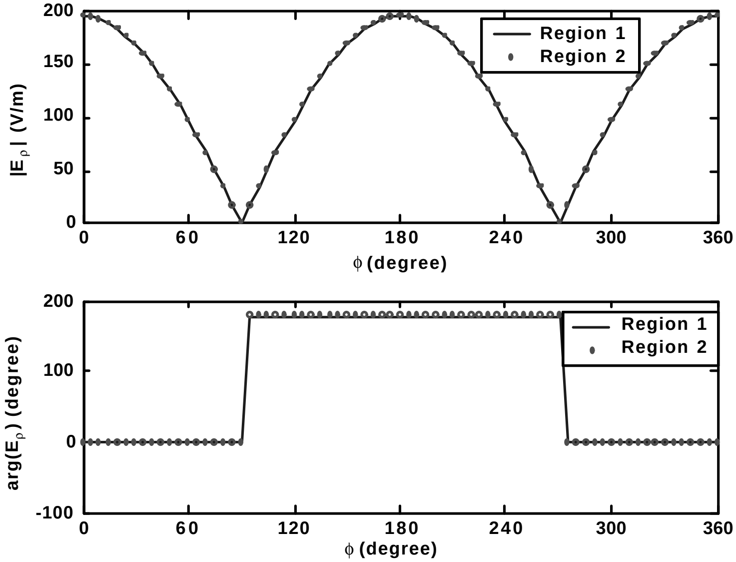

(a) $E_\rho \, (\rho = a - \tau)$

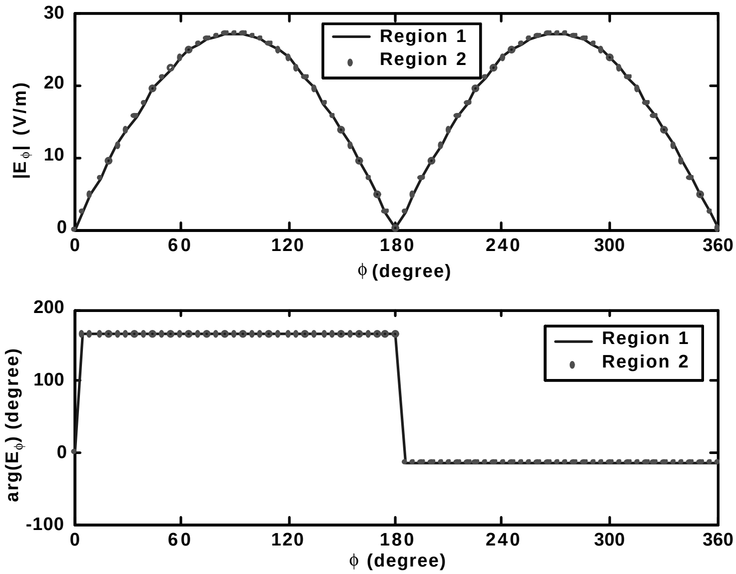

(b) $E_\phi \, (\rho = a - \tau)$

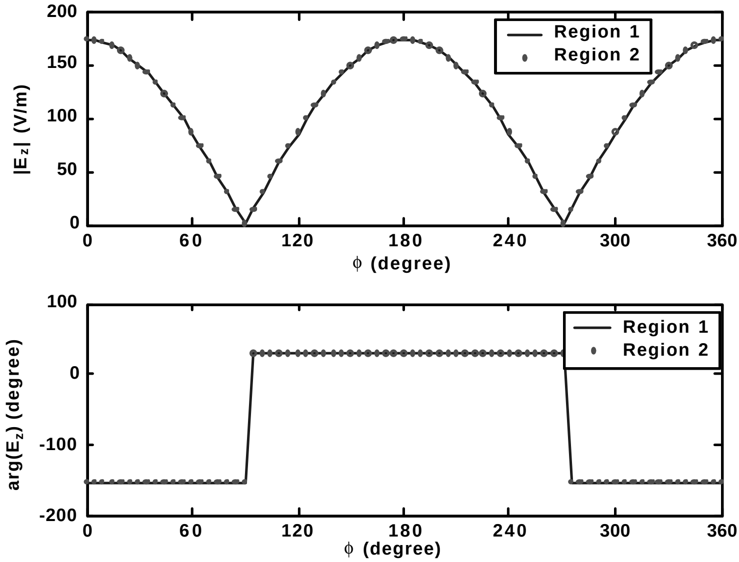

(c) $E_z\,(\rho = a - \tau)$

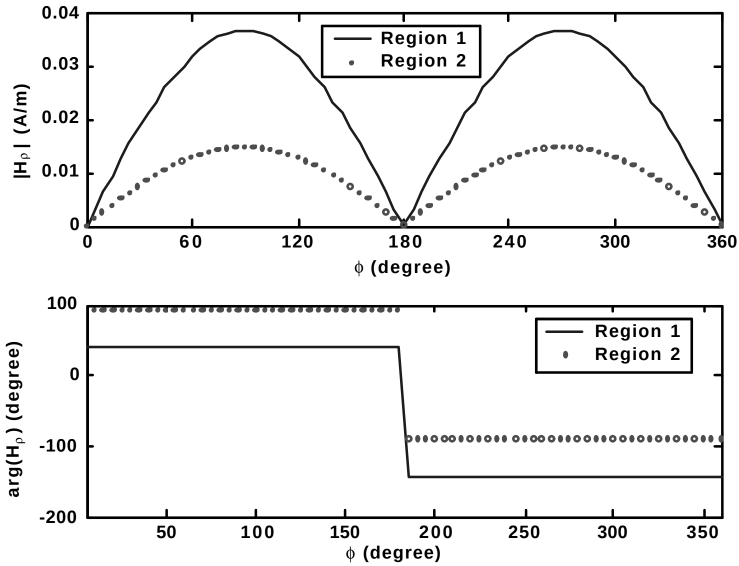

(d) $H_\rho\,(\rho = a - \tau)$

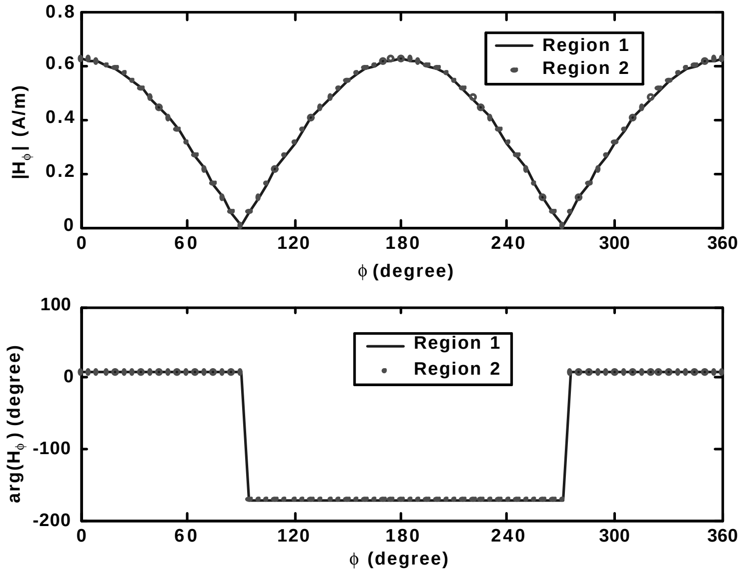

(e) $H_\phi\,(\rho = a - \tau)$

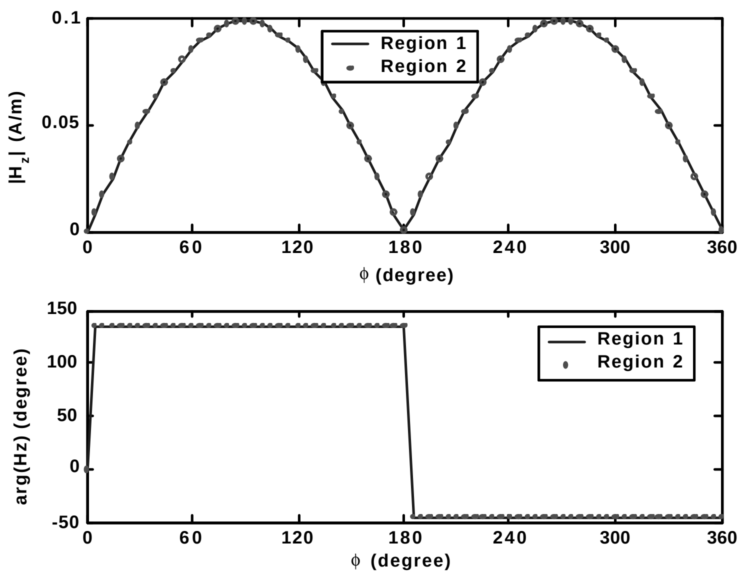

(f) $H_z\,(\rho = a - \tau)$

Figure 11. The fields of the EH_{11} mode at the interface between the two layers.

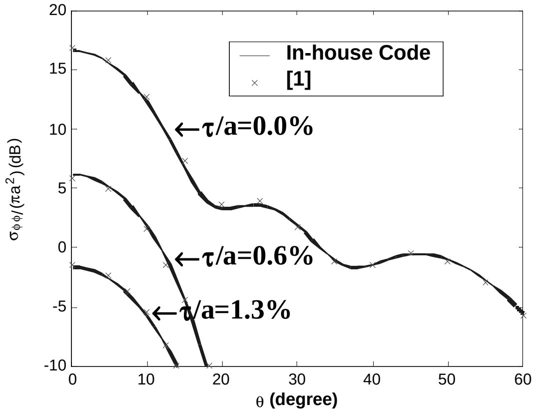

(a) $\theta\theta$ Polarization

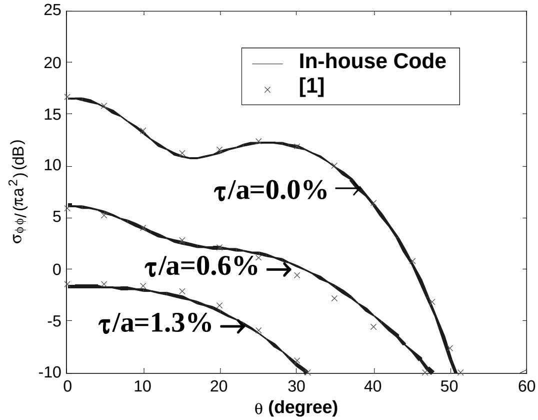

(b) $\phi\phi$ Polarization

Figure 12. The echo area of a PEC-terminated circular waveguide coated with a lossy material: $a = 3.9525\,\text{cm}$, $f = 9.2\,\text{GHz}$, $L = 26.46\,\text{cm}$, $L1 = 1\,\text{cm}$, $\varepsilon_r = 12 - j0.144$, $\mu_r = 1.74 - j3.306$.

It is observed from Figs. 8–10 that there are slight differences between the results published in [12] and those obtained using our in-house code. In order to verify the results obtained using our in-house code, the phase and amplitude of the six field components of the EH_{11} mode at the interface between two layers are calculated and plotted in Fig. 11 for a coated circular waveguide with $\tau/a = 4\%$, $a/\lambda = 1.4433$. From Fig. 11, it is clearly observed that the phase and amplitude of all tangential fields match very well at the interface between the two layers. This verifies the correctness of the present method and our in-house code.

The scattering from the coated circular waveguide has also been simulated. Figure 12 shows the echo area of the structure shown in Fig. 6 with $a = 3.9525\,\text{cm}$, $f = 9.2\,\text{GHz}$, $L = 26.46\,\text{cm}$, $L1 = 1\,\text{cm}$, $\varepsilon_r = 12 - j0.144$, $\mu_r = 1.74 - j3.306$. It is observed that the results obtained by our in-house code are in good agreement with that published in [1] and the coating material can significantly reduce the echo area of circular waveguide.

5. CONCLUSIONS

In this paper, the characteristic equation is modified via the application of the Hankel function of the second kind, instead of Bessel function of the first kind in the layer i ($i \geq 2$). The modified characteristic equation enables us to smoothly and accurately determine the propagation constants in any coated circular waveguide numerically. This allows us to predict correctly the scattering from the circular coated waveguide.

REFERENCES

1. Lee, C. S. and S. W. Lee, "RCS of a coated circular waveguide terminated by a perfect conductor," *IEEE Trans. Antennas Propagat.*, Vol. 35, 391–398, April 1987.
2. Anastassiu, H. T., J. L. Volakis, and D. C. Ross, "The mode matching technique for electromagnetic scattering by cylindrical waveguides with canonical terminations," *J. Electromagn. Waves Appl.*, Vol. 9, 1363–1391, No. 11/12, 1995.
3. Moll, J. W. and R. G. Seecamp, "Calculation of radar reflecting properties of jet engine intakes using a waveguide model," *IEEE Aerospace and Electronic Systems*, Vol. AES-6, 675–683, Sep. 1970.
4. Altintas, A., P. H. Pathak, and M. C. Liang, "A selective modal scheme for the analysis of EM coupling into or radiation from large open-ended waveguides," *IEEE Trans. Antennas Propagat.*, Vol. 36, 84–96 , Jan. 1988.
5. Ling, H., S. W. Lee, and R. C. Chou, "High-frequency RCS of open cavities with rectangular and circular cross sections," *IEEE Trans. Antennas Propagat.*, Vol. 37, 648–654, May 1989.

6. Ling, H., R. C. Chou, and S. W. Lee, "Shooting and bouncing rays: calculation RCS of an arbitrarily shaped cavity," *IEEE Trans. Antennas Propagat.*, Vol. 37, 194–205, Feb. 1989.
7. Burkholder, R. J., "High-frequency asymptotic methods for analyzing the EM scattering by open-ended waveguide cavities," Thesis (Ph.D.), Ohio State University, 1989.
8. Rodríguez, J. L., F. Obelleiro, and A. G. Pino, "Iterative solutions of MFIE for computing electromagnetic scattering of large open-ended cavities," *IEE Proc. — Microw. Antennas Propag.*, Vol. 144, No. 2, 141–144, April 1997.
9. Wang, T. M. and H. Ling, "Electromagnetic scattering from three-dimensional cavities via a connection scheme," *IEEE Trans. Antennas Propagat.*, Vol. 39, 1505–1513, Oct. 1991.
10. Trintinalia, L. C. and H. Ling, "Electromagnetic scattering from 3-D arbitrary coated cavities via a connection scheme using triangular patches," *J. Electromagn. Waves Appl.*, Vol. 8, 1411–1423, No. 11, 1994.
11. Jin, J. M., "Electromagnetic scattering from large, deep, and arbitrarily-shaped open cavities," *Electromagn.*, Vol. 18, 3–34, 1998.
12. Chou, R. C. and S. W. Lee, "Modal attenuation in multilayered coated waveguides," *IEEE Trans. Microwave Theory Tech.*, Vol. 36, 1167–1176, July 1988.
13. Harrington, R. F., *Time-Harmonic Electromagnetic Fields*, McGraw-Hill, New York, 1961.
14. Yeh, C. and G. Lindgren, "Computing the propagation characteristics of radially stratified fibers: an efficient method," *Appl. Optics*, Vol. 16, 483–493, Feb. 1977.
15. Collin, R. E., "The optimum tapered transmission line matching section," *Proc. IRE*, Vol. 44, 539–548, Apr. 1956.
16. Unger, H., "Circular waveguide taper of improved design," *Bell System Tech. J.*, Vol. 37, 899–912, July 1958.

Fu-Gang Hu was born in October 1977, Jiangxi, P. R. China. He received B.Eng. and M.Eng. degrees from Xidian University, Xi'an, P. R. China, in 1999 and 2002, respectively. He has been an Associate Scientist with Temasek Laboratories, National University of Singapore, Singapore, since 2002. His current research interest includes electromagnetic modeling using numerical techniques.

Chao-Fu Wang received the B.Sc. degree in mathematics from the Henan Normal University, Xinxiang, China, in 1985, the M.Sc. degree in applied mathematics from the Hunan University, Changsha, China, in 1989, and the Ph.D. degree in electrical engineering from the University of Electronic Science and Technology of China, Chengdu, China, in 1995, respectively. From 1987 to 1996, he was a Lecturer, and then an Associate Professor of the Department of Applied Mathematics at the Nanjing University of Science and Technology (NUST). Since February 1996, he has been an Associate Professor of the Department of Electronic Engineering at the NUST. From 1996–1999, he was a Postdoctoral Research Fellow in the Center for Computational Electromagnetics (CCEM), University of Illinois at Urbana-Champaign (UIUC). From 1999–2001, he was a Research Fellow in the Department of Electrical and Computer Engineering, National University of Singapore (NUS). He is currently a Research Scientist and Project Leader in the Temasek Laboratories, NUS. His current research interests include fast algorithms for computational electromagnetics, scattering and antenna analysis, ferrite components and their analysis, MMIC design and simulation.

Yuan Xu received the B.S., M.S. degrees in mathematics from Suzhou University, P. R. China, and Ph.D. degrees in electromagnetic theory and microwave technology from Nanjing University of Science and Technology, P. R. China, in 1988, 1991, and 2001, respectively. He is currently a Research Scientist in the Temasek Laboratories, National University of Singapore. From 1991 to 1999, he was with Department of Applied Mathematics, Nanjing University of Science and Technology. From May 1999 to September 2000, he was a research assistant in Department of Electric Engineering, City University of Hong Kong. His research interests include computational electromagnetics, integral equation methods, and analysis of large-scale electromagnetic radiation and scattering problem.

Yeow-Beng Gan received the B.Eng. (Hons) and M.Eng. degrees in electrical engineering from the National University of Singapore, Singapore, in 1989 and 1994, respectively. He has been with the DSO National Laboratories (formerly the Defence Science Organisation) since 1989, and was primarily responsible for the build-up of technical capabilities in the analysis and design of antennas in DSO. He became a Principal Member of Technical Staff in 1998, in the area of electromagnetics and antennas. In May 2001, he was seconded to the Temasek Laboratories, National University of Singapore, where he is currently a Principal Research Scientist. His research interests include periodic arrays for antennas and radomes, wave physics, computational electromagnetics, and modeling of composite materials.